ELSEVIER

International Journal of Pharmaceutics 230 (2001) 11–24

international journal of pharmaceutics

www.elsevier.com/locate/ijpharm

pH-sensitive nanoparticles of poly(amino acid) dodecanoate complexes

Sascha General [a,*], Andreas F. Thünemann [b,c]

[a] *Max Planck Institute of Colloids and Interfaces, Am Mühlenberg, D-14476 Golm, Germany*
[b] *Fraunhofer Institute for Applied Polymer Research, Geiselbergstrasse 69, D-14476 Golm, Germany*
[c] *Institute of Theoretical Physics II, Heinrich Heine University Düsseldorf, Universitätsstr. 1, D-40225 Düsseldorf, Germany*

Received 20 April 2001; received in revised form 19 July 2001; accepted 19 July 2001

Abstract

Nanoparticles were formed by the complexation of poly(L-arginine) (PLA), poly(L-histidine) (PLH) and poly(L-lysine) (PLL) with dodecanoic acid (C12). Dynamic light scattering, ζ potential measurements, atomic force microscopy, fluorescence, and circular dichroism spectroscopy were used for their characterization. It was found that the diameters of the poly(L-arginine) dodecanoate (PLA-C12), poly(L-histidine) dodecanoate (PLH-C12), and poly(L-lysine) dodecanoate (PLL-C12) complex nanoparticles were in the range 120–200 nm. Furthermore, the pH-sensitive dissolution and the surface charges can be adjusted by choosing PLA, PLH and PLL. The particle stability against basic pH values increases with increasing pK_a value of the poly(amino acid) in the series PLH-C12, PLL-C12 and PLA-C12. The particles as such show a core-shell morphology. Their cores are formed by stoichiometric poly(amino acid) dodecanoate complexes while the shells stabilizing the particles are formed by cationic poly(amino acid) chains in an uncomplexed state. The particles were tested as containers for hydrophobic molecules such as pyrene, which served as a fluorescence probe for measuring the polarity within the particles, and Q_{10} which functioned as a model drug. The maximum uptake of Q_{10} into the nanoparticles is about 13% (w/w), thereby making the complexes attractive as simple drug carriers for controlled release purposes. Circular dichroism measurements revealed that the poly(amino acid) chains of PLA-C12 and PLL-C12 adopt predominantly an α-helix and that of PLH-C12 a β-sheet.

Keywords: pH-sensitive; Nanoparticles; Poly(amino acids); Self-assembly; Secondary structure

1. Introduction

The immobilization of pharmacological active compounds by their complexation with polyelectrolytes has been a subject of intense research, in particular related to the complexation of DNA (Byk and Sherman, 2000). Poly(amino acid)s, such as PLL, are frequently utilized cationic polymers in gene delivery investigations (Seymour et al., 1999; Ramsay et al., 2000). Evidence accumulated to date indicates that poly(ethylene imine)

* Corresponding author. Tel.: +49-331-567-9538; fax: +49-331-567-9502.

0378-5173/01/$ - see front matter
PII: S0378-5173(01)00829-8

homopolymers complexed with DNA provide a high degree of transfection when compared with optimized cationic liposome formulations or with poly(amino acid)-DNA complexes (Boussif et al., 1995; Remy et al., 1998). Recent publications, discussing colloidal dispersions, introduced these composites as suitable carriers for pharmacological active substances of low molecular weight in pharmaceutical applications. Block-*co*-polymers, for example, poly(ethylene oxide)-*block*-poly(L-lysine)s have been used to immobilize retinoic acid (Thünemann and General, 2000). Another recent approach for drug delivery purposes is to combine the encapsulation of drugs with lipids and polymers using mixtures of liposomes and polyelectrolytes (Gao and Huang, 1996; Nakamura and Osanai, 2000; Kawashima et al., 2000).

It was an important finding that the electrostatic interactions of polyelectrolyte complexes are switchable by changing the pH value of the surrounding media (Tirrell and Linhardt, 2000) in a way that the complexes can be dissolved. Incorporated drugs are released easily when these complexes dissolve. Further, the pH dependent release, particularly the endosomal release of therapeutically used molecules via membrane fusion or the destabilization of pH sensitive liposomes, has been studied extensively (reviewed in Drummond et al., 2000).

The aim of our study is to design nanoparticles formed by poly(amino acid) homopolymers and dodecanoic acid (C12) as relatively simple containers suitable for the incorporation of hydrophobic drugs. C12 was chosen because it is a natural medium chain fatty acid (Muraoka et al., 2000) and found to be appropriate for the complexation of poly(ethylene imine) (Thünemann and General, 2001). Accordingly, C12 was assumed to be useful for the complexation of the cationic homopolymers poly(L-lysine) (PLL), poly(L-arginine) (PLA) and poly(L-histidine) (PLH). These poly(amino acid)s were selected because they are easily accessible and, in principle, biocompatable. For clarity the chemical structures of all compounds are shown in Fig. 1. The complexes used in this study were prepared in analogy to poly(ethylene imine) dodecanoate complexes (Thünemann and General, 2001), using a 2:1 stoichiometry of polymer to C12 which is an optimum for particle formation. The same stoichiometry was used here for PLA-C12, PLH-C12 and PLL-C12. Our study further investigated the dependency of the complex stability as a function of the pK_a values of the poly(amino acid)s.

2. Materials and methods

2.1. Materials

Poly(L-arginine) hydrochloride ($M_w = 36400$ g mol^{-1}), poly(L-histidine) hydrochloride ($M_w =$

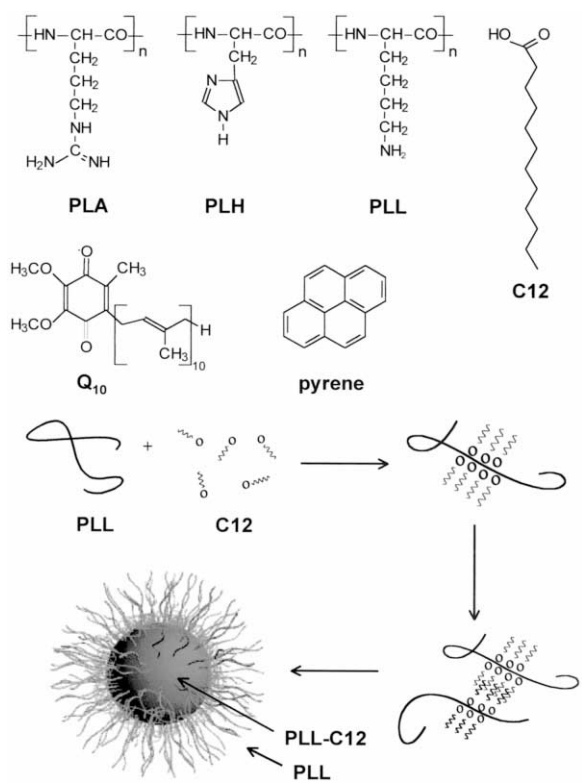

Fig. 1. Chemical structures of the building blocks for the formation of the nanoparticles: poly(L-arginine) (PLA), poly(L-histidine) (PLH), poly(L-lysine) (PLL) and dodecanoic acid (C12). The hydrophobic molecules Q_{10} and pyrene were used for testing the carrier properties of the nanoparticles. The lower figure is a sketch of a possible formation mechanism of the nanoparticles. First, block-like structures of partially complexed poly(amino acid) chains are formed. Second, these block-like structures aggregate and finally form core-shell particles with a shell of uncomplexed poly(amino acid) segments.

15000 g/mol), poly(L-lysine) hydrobromide ($M_w = 29800$ g/mol), dodecanoic acid ($> 99.5\%$), sodium hydroxide, hydrochloric acid, pyrene, Q_{10} (ubiquinone 50), and tetrahydrofuran (THF, HPLC grade) were supplied by Sigma/Aldrich and used as received. The purity of the dodecanoic acid was checked by determining its melting point and melt enthalpy by using differential calorimetry. It was found that the melting point (44.2 °C) and the melt enthalpy (36.7 kJ mol^{-1}) are identical to the data reported in the literature (Small, 1986).

2.2. Nanoparticle preparation

A total of 40 ml of a 2 mmol l^{-1} solution of the three poly(amino acid)s in distilled water were used for nanoparticle preparations. The stoichiometries were calculated with respect to the charges. Then 4 ml of an aqueous 10 mmol l^{-1} solution of the dodecanoic acid (pH adjusted to 9.5 with sodium hydroxide) were slowly added to each of the solutions. Nanoparticles of PLA-C12, PLH-C12 and PLL-C12 complexes were immediately obtained as opaque solutions, stirred for 60 min at a temperature of 25 °C and filtered by using a 800 nm membrane filter. The pH was adjusted to 6.5 with diluted hydrochloric acid.

2.3. Incorporation of model compounds

For the incorporation of the model compounds, 3.4 mg of Q_{10} dissolved in 8 ml THF and 0.3 mg of pyrene dissolved in 10 ml of THF were added to the dodecanoate solution before mixing it with the polymer solutions. The solutions obtained were stirred slowly (1–2 s^{-1}) at 35 °C for 24 h to remove the THF (evaporation method, Ferdous et al., 1998). The evaporated water was replaced and the dispersions of the complexes were filtered using a 800 nm membrane filter.

2.4. Methods

The size of the nanoparticles was determined by dynamic light scattering, using a fixed angle (90 °) Nicomp 370 submicron particle sizer. The samples were loaded into the measuring cell at a concentration (usually 100 mg/l) that yields an optimum signal output (current count rate, 300 kHz). Intensity-averaged size was derived by using the Nicomp distribution analysis provided by version 12.0 of the Nicomp software. The number of replicants was five. The standard deviations of the particle size distributions were $\sim 13\%$ of their mean sizes. The ζ potentials of the nanoparticles were determined with a Zetamaster (Malvern Instruments) averaging five measurements. The same solutions were used for dynamic light scattering and ζ potential measurements. The scanning force microscopy was performed with a Nano Scope IIIa microscope (Digital Instruments, Santa Barbara, CA), operating in tapping mode. The instrument was equipped with a 10×10 μm E-scanner and commercial silicon tips (model TESP, the force constant was 50 N/m, the resonance frequency was 300 kHz, and the tip radius was < 20 nm). The samples were prepared by letting droplets of diluted aqueous solutions (100 mg/l) dry on freshly cleaved muscovite mica surfaces at room temperature. The differential scanning calorimetry measurements were performed on a Netzsch DSC 200. Each sample was examined at a scanning rate of 10 K min^{-1} by applying two heating scans and one cooling scan. The onset of the exothermic peak in the second heating cycle was used to determine the melting transition. Analytical ultracentrifugation was carried out using a Beckman Optima XL-I ultracentrifuge (Beckman Counter, Palo Alto, CA) at 25 °C and 5000, 20000 and 60000 rpm (2000, 31 800 and $286\,000 \times g$). Detection of the particles was carried out by applying UV-vis absorption detection at wavelengths of 285 and 400 nm and simultaneously with the Raleigh interference optics. The luminescence of complexes was analyzed using a Perkin-Elmer LS-50B luminescence spectrometer. Emission spectra were collected in the range 350–500 nm with an excitation wavelength of 335 nm and slits of 2.5/2.5 nm. Circular dichroism was detected by a spectropolarimeter (J715 from Jasco, Gross-Umstadt). The measurements were performed in the far-UV range (190–260 nm).

Table 1
Sizes of the PLA-C12, PLH-C12, PLL-C12 nanoparticles, their ζ potentials and the pK_a values of the side chains of the poly(amino acid)s

Complex	Particle diameter [nm]	ζ potential [mV]	pK_a of side chains[a]
PLA–C12	180 ± 25	67 ± 7	12
PLH–C12	200 ± 25	42 ± 7	6.5–7.0
PLL–C12	205 ± 15	59 ± 7	10.0–10.2

[a] Goddard and Ananthapadmanabhan (1993).

3. Results and discussion

3.1. Particle characterization

The addition of C12 to the poly(amino acid) solutions results in the spontaneous formation of nanoparticles, even if the concentration of C12 is an order of magnitude below its critical micelle concentration at 2.8×10^{-2} mol l^{-1} (Goddard and Ananthapadmanabhan, 1993). This is characteristic for the formation of polyelectrolyte-surfactant complexes, which occur typically at surfactant concentrations up to three orders of magnitude lower than the CMC of the surfactant (Goddard, 1986; Watanabe et al., 1996). The mean diameters of the nanoparticles obtained of PLA-C12, PLH-C12 and PLL-C12 were in the range of 180–205 nm with standard deviations of ± 15 to ± 25 nm (Table 1). A significant change of the particle sizes could not be observed when changing the temperature during the particle formation in the range of 20 to 45 °C and while the sheering rate of the stirrer was between 1 and 10 s^{-1}. A macroscopic precipitation of the complexes was observed, for example, when the solutions were boiling during the particle formation. Interestingly the particles of the three complexes did not differ in their sizes. A similar effect was reported earlier for the preparation of particles formed by polyelectrolyte complexes whose sizes at low salt concentrations are independent of the type of the polyelectrolytes (Buchhammer et al., 1999). In addition particles with constant diameters of ~ 120 nm were found for nanoparticles of poly(ethylene imine)-DNA complexes (Hellweg et al., 2000). Other investigations have also shown that there is a preferred diameter of the particles formed by complexes depending on the polyelectrolyte and the counter ion size (Bloomfield, 1991; Tang and Szoka, 1997). When a 1–1 stoichiometry of poly(amino acid) to C12 was approached, precipitation of the charge neutralized complexes was observed as is typically found for many polyelectrolyte-surfactant complexes (Antonietti et al., 1994). It is not yet clear what determines the particle size of the different complexes, but kinetical components are likely to play a major role. For example, when reducing the concentrations of the poly(amino acid)s from 2.0 to 0.4 mmol l^{-1}, while keeping the stoichiometries constant, a reduction of the resultant particle sizes from 200 to $\sim 120 \pm 30$ nm was observed. By contrast, the particle sizes remained constant when the solutions of the complexes were diluted after complex formation. Taking into account that the sizes of the nanoparticles depend significantly on their preparation conditions, but not on the dilution of the dispersions, it was concluded that these nanoparticles are kinetically stable. By analogy to non-equilibrium structures of block copolymers in aqueous solution (Jada et al., 1996) the poly(amino acid)-C12 complex nanoparticles may be characterized as so-called 'frozen micelles'. Once these kinetically stable aggregates are formed they do not change in size or composition while diluting the dispersion due to the hindered exchange dynamics of single molecules and aggregates. The same trend, namely the observation of smaller particle sizes at lower concentrations of the compounds at preparation, was obtained in our previous investigation on poly(ethylene imine)-C12 complex particles (Thünemann and General, 2001). In the case of poly(ethylene imine)-C12 the particles were stabilized by an

excess of poly(ethylene imine) above a 1:1 stoichiometry. The excessive poly(ethylene imine) molecules form a cationic corona which protects the charge neutralized cores of the particles from precipitation.

ζ potential measurements were carried out in order to investigate the type of stabilization of the poly(amino acid)-C12 nanoparticles. The ζ potentials were 67 ± 7 mV (PLA-C12), 42 ± 7 mV (PLH-C12) and 59 ± 7 mV (PLL-C12) at a pH of 6.5. Obviously the ζ potentials correlate to the pK_a values of the amino acid side chains, which are ~ 12 (PLA), 6.5–7.0 (PLH) and 10.0–10.2 (PLL), when they are attached to poly(amino acid)s (cf. Goddard and Ananthapadmanabhan, 1993). The data is summarized in Table 1. The ζ potentials of the nanoparticles are unusually high when compared, for example, with PLL coated poly(ε-caprolactone) nanocapsules showing a ζ potential of ~ 30 mV (Calvo et al., 1997). But ζ potentials as high as 60 mV and higher have already been reported in adsorption measurements on charged surfaces using poly(diallyldimethylammonium chloride) with a molar mass of $\sim 2.4 \times 10^5$ g/mol (Schwarz et al., 1998). The high ζ potentials of the poly(amino acid)-C12 complexes indicate that the surfaces of the nanoparticles are covered with uncomplexed poly(amino acid)s as a stabilizing shell.

Scanning force microscopy measurements were carried out on dispersions dried on a negatively charged mica surface in order to reveal the morphologies of the particles. A typical topography picture of the PLL-C12 complex nanoparticles can be seen as an example in the insert in Fig. 2, which resembles two 'fried eggs'. It can be seen there that the two particles are of a core-shell type. The cores appear bright and seem to be relatively compact while the shells appear relatively diffuse. The height profile of the particles along the straight line in the insert is represented by the graph in Fig. 2. Further, the cores, each having a height of 12 nm and a diameter of ~ 100

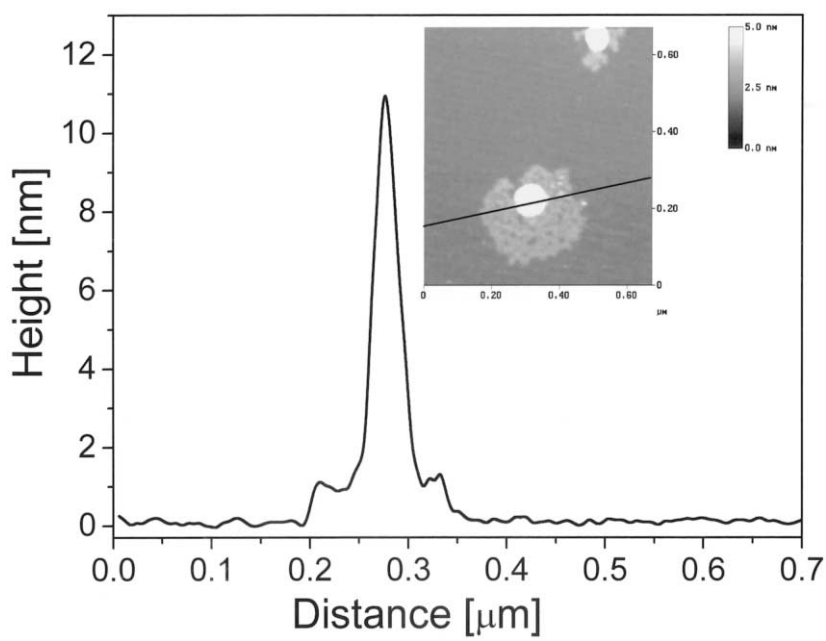

Fig. 2. AFM image of PLL-C12 core-shell nanoparticles dried on mica surfaces (insert). The lower curve displays the height profile of a single particle along the solid line in the insert.

nm, have the typical profile of well-defined particles that flatten during drying. By contrast the elevation of the shells is <1 nm above the mica surface. We suppose that the cores are formed by a PLL-C12 stoichiometry of nearly 1:1 and that they interact only weakly with the mica. The shells, on the other hand, contain uncomplexed PLL that interacts strongly with the mica. It therefore seems to be justified to conceive the particles of core-shell morphology. AFM images of the two other poly(amino acid)-C12 complex particles showed no differences in the particle morphologies, revealing that the conformation of the poly(amino acid)s had no influence.

We propose two limiting mechanisms for creating the core-shell particles with a stabilizing poly(amino acid) shell. In the first mechanism single poly(amino acid) chains are complexed to a 1:1 stoichiometry. These complexed chains then assemble to larger hydrophobic domains. If these hydrophobic domains reach a certain-concentration dependent-size they act as deposition sites for uncomplexed poly(amino acid) chains which are still in solution after all dodecanoate ions are complexed. These poly(amino acid) chains deposit onto the surfaces of the hydrophobic domains, forming stabilizing cationic shells, which stop further aggregation of hydrophobic domains. The shell-forming step can be considered similar to that found for protein-polyelectrolyte core-shell particles prepared by stepwise layer adsorption techniques (Caruso and Möhwald, 1999). Oppositely charged polyelectrolytes and fluorescein isothiocyanate-labeled bovine serum albumin and immunoglobulin G were adsorbed on polystyrene latex particles in an alternating fashion forming uniformly coated colloids.

In the second mechanism the formation of macromolecular amphiphiles is the first step. The aggregation of partially complexed chains starts before the poly(amino acid) chains are fully complexed. This means that for a limited time during the complexation a partially complexed poly(amino acid) chain appears like a block copolymer chain with a hydrophilic and a hydrophobic block. The hydrophobic block is represented by a poly(amino acid)-C12 section and the hydrophilic block by an uncomplexed poly(amino acid) section. Then the hydrophobic blocks aggregate to hydrophobic domains, that are surrounded by the uncomplexed cationic chains. This also results in core-shell particles. Obviously complexation and aggregation are in competition and the particle sizes therefore depend on the concentrations during preparation. It is likely that a combination of these limiting mechanisms is close to the experimental particle formation mechanism. The complexation itself, in both particle formation mechanisms, is a zipper mechanism, based on the finding that the preferred complexation binding site along a polyelectrolyte chain is the next closest position to an occupied site. The initiation of the zipper mechanism is caused by hydrophobic interactions of the alkyl tails of dodecanoic acid (e.g. Philipp et al., 1982; Hayagawa et al., 1983). A Sketch of the particle formation is given in Fig. 1.

3.2. Saline stability

The saline stability of the nanoparticles is of interest when evaluating their possible utility as drug carriers. One can expect that the highly positively charged nanoparticles aggregate after the addition of sodium chloride due to a reduction of their charge stabilization. Therefore their diameters at different salt concentrations were investigated. It was observed that the particles of PLA-C12, PLH-C12 and PLL-C12 are stable, at least in sodium chloride solutions of concentrations up 0.25 mol l^{-1}, and for a period of 30 days. This concentration is considerably higher then that of a physiological sodium chloride solution (0.15 mol l^{-1}). For comparison the data is summarized in Fig. 3. From the increase of the particles sizes at the highest salt concentrations (>0.4 mol l^{-1}) it can be tentatively assumed that the salt stability increases slightly in the line PLA-C12, PLH-C12, PLL-C12.

3.3. pH stability

A major aim of this study is to cause the dissolution of the nanoparticles by varying the pH value. Therefore the pH value of their surroundings was adjusted by using hydrochloric acid and

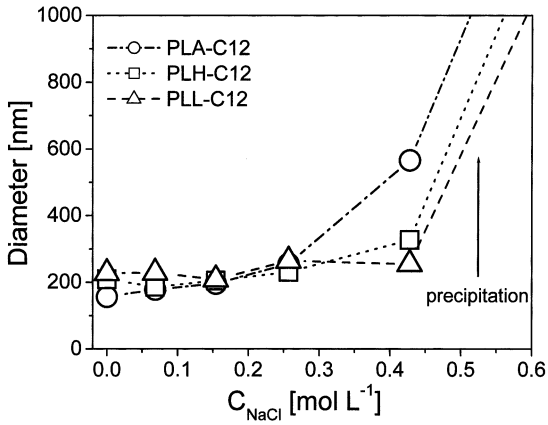

Fig. 3. Diameters of the PLA-C12 (circles), PLH-C12 (squares) and PLL-C12 nanoparticles (triangles) in sodium chloride solutions as determined by dynamic light scattering.

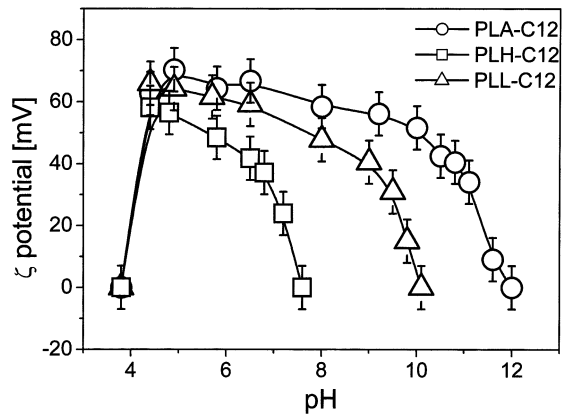

Fig. 5. ζ potentials of the PLA-C12 (circles), PLH-C12 (squares) and PLL-C12 nanoparticles (triangles) as a function of the pH values. The lines are plotted to guide the eye.

sodium hydroxide. After that we determined the particle diameters as well as their ζ potentials. The results are shown in Figs. 4 and 5. It can be seen in Fig. 4 that the PLA-C12 nanoparticles are stable in the pH range of 4.3–11, the PLH-C12 in the range of 4.3–6.8, while the PLL-C12 is stable in the range of 4.3–9.8. This means that the stabilization limit at higher pH values is roughly determined by the pK_a values of the poly(amino acid)s while the stability at lower pH values is close to the pK_a value of dodecanoic acid (Table 1). The sizes of the particles were constant, at least for 2 days after changing the pH value. A precipitate of white crystals was obtained for all complexes below a pH value of 4.3. It was formed from pure dodecanoic acid as revealed by DSC measurements. In addition, no particles of submicron size were detected in the remaining solutions below a pH of 4.3. This indicates that the nanoparticles were completely broken down into their compounds. Although the pK_a value of alkyl carboxylic acids is 4.9 or higher (Small et al., 1986) all complexes were stable down to a pH of 4.3. At this pH, according to the Henderson-Hasselbalch equation, only 20% of the carboxylic functions are in an ionic state and can therefore bind electrostatically to the poly(amino acid)s. This means that not all of the C12 molecules in the complexes have to be in their deprotonated state in order to maintain the stability of the nanoparticles. Obviously, the break-down of the particles in the lower pH region is independent of the poly(amino acid), as it had been expected.

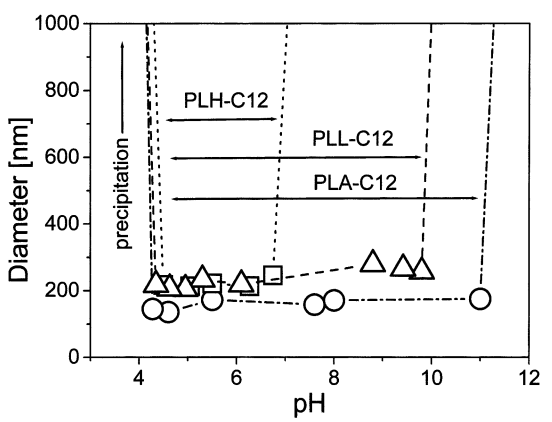

Fig. 4. Diameters of the PLA-C12 (circles), PLH-C12 (squares) and PLL-C12 nanoparticles (triangles) as a function of the pH values. The arrows indicate the range in which discrete particles were observed. Lines are plotted to guide the eye.

The situation is different, however, in the region of higher pH values. It can be seen in Fig. 4 that the PLA-C12 particles are stable up to a pH value of 11.1, the PLH is stable up to 6.8 and the PLL-C12 up to 9.9. Above these values the complexes aggregate. No residue remained after filtration (800 nm cutoff size). This indicates that the complexes were precipitated quantitatively at the regions of high pH values. The pH dependent

stability regions of the particles are depicted by arrows in Fig. 4.

In addition to the particle size measurements we recorded the ζ potentials of the particles at different pH-values (Fig. 5). It was observed that the particles display positive ζ potentials dropping sharply towards zero on the lower pH side, while they decrease smoothly on the side of higher pH values. The nanoparticles dissolve at a pH below 4.3 due to the potonation of C12, which is independent of the poly(amino acid). Accordingly the ζ potentials drop sharply. By contrast, the decrease to zero at higher pH values depends strongly on the poly(amino acid). The ζ potential decreases in the line PLH-C12, PLL-C12, PLA-C12 according to the increase of the pK_a values. The zero values of the ζ potentials in the region of higher pH values were found at pH 7.6 (PLH-C12), 10.1 (PLL-C12) and 12.0 (PLA-C12), which are close to the values above for which the aggregation of the particles was observed. The particles with ζ potentials below $+20$ mV were found to be unstable (cf. particle sizes). They start to aggregate after 30 min. The highest ζ potentials were found at relatively low pH values. At pH 4.7 the particles derived from the PLA-C12 complex exhibited the highest observed ζ potential (70.3 mV) found in this study.

3.4. Q_{10} doped nanoparticles

We incorporated up to 13% [w/w] of Q_{10} into the hydrophobic domains of the particles (Section 2.3). No differences in their sizes or their size distributions were found between pristine and Q_{10} doped PLA-C12, PLH-C12 and PLL-C12 nanoparticles when using dynamic light scattering. The sizes of the particles were found to be constant for a period of at least 30 days. No precipitation was observed. The UV spectra of the dispersion was constant in height and shape, presenting the typical absorption maximum of Q_{10} at $\lambda = 272$ nm. Filtration of the dispersion through a 800 nm filter had no significant effect on the particle sizes and the UV spectra. Therefore we can exclude larger aggregates of crystalline Q_{10}. Analytical ultracentrifugation measurements were used as a further test to reveal that the Q_{10} is dissolved in the nanoparticles. The sedimentation profiles of pristine particles were determined at first by using an interference optic and an UV detector (detection of 285 nm). The maxima of the sedimentation coefficients were found to be in the range of 70×10^{-13}–90×10^{-13} s^{-1}. Relatively broad distributions (standard deviations of $\sim 20 \times 10^{-13}$ s^{-1}) indicated that the particle size distributions were broad as was expected from the results of the dynamic light scattering measurements.

The experiments were repeated with nanoparticles doped with Q_{10}. It was found that the doped particles were UV active at 400 nm, while the pristine particles were inactive at this wavelength. The determination of the sedimentation coefficients of the doped particles was carried out as for the pristine particles and, additionally, at a wavelength of 400 nm. The same range of sedimentation coefficients was found for doped and non-doped particles. Therefore the results of UV-vis spectroscopy, dynamic light scattering and ultracentrifugation are therefore consistent with the interpretation that the Q_{10} is dissolved homogeneously in the nanoparticles. The next question was how to get information about the surroundings of hydrophobic molecules within the nanoparticles.

3.5. Pyrene fluorescence

Fluorescent molecules, in particular pyrene, have been widely used to probe the microenvironments of organized host media such as polyelectrolyte complexes (Caruso et al., 1998). Pyrene has the ability to measure the polarity of its microenvironment. This makes it useful for gaining information about the nanoparticles as carriers for typical hydrophobic compounds. The pyrene was incorporated in the nanoparticles in the same way as Q_{10} to confirm the incorporation of the model compound. In order to obtain information on how the pyrene is located, steady-state fluorescence measurements on pyrene-doped nanoparticles of the complexes were carried out. The $\pi \rightarrow \pi^*$ emission spectrum of monomer pyrene exhibits five major vibration bands between 370 and 400 nm, labeled I–V. The vibra-

tion bands I and III are located at wavelengths of 372.4 and 382.9 nm. It is known that the peak of I shows a significant decrease in its intensity compared with peak of III when the polarity of the surroundings of the pyrene decrease. Thus the ratio of the emission intensities of the vibration bands I and III (I_I/I_{III}) serves as a measure for the polarity of the surroundings of pyrene. For example, the I_I/I_{III} ratio is 1.02 to 1.13 in *n*-butanol and 1.69–1.87 in water (Kalyanasundaram and Thomas, 1977; Dong and Winnik, 1982; Tedeschi et al., 2001) Dipole-induced interactions (Ham effect) between pyrene and its microenvironment are responsible for the changes in the intensity ratio I_I/I_{III} (Mast and Haynes, 1975; Hollas et al., 1998).

3.6. The I_I/I_{III} ratios of the nanoparticles as a function of the pH values are plotted in Fig. 6

It can be seen there that the I_I/I_{III} ratios follow a comparable trend as found for the ζ potentials. The I_I/I_{III} ratios have their lowest values at pH 4.5 (1.00–1.05) for all complexes. This is attributed to a semipolar microenvironment that can be identified as the cores of the nanoparticles. It can be seen in Fig. 6 that the peak ratios increase sharply to values of 1.65–1.70 for all the complexes when the pH was reduced to 3.8. These values are close to that of pure water and result from a strong increase in the polarity of the pyrene microenvironment. We interpret this finding as a consequence of the dissolving of the nanoparticles accompanied by a release of pyrene when the pH is reduced form 4.3 to 3.8. This is consistent with the results of the measurements of the particle sizes and the ζ potentials.

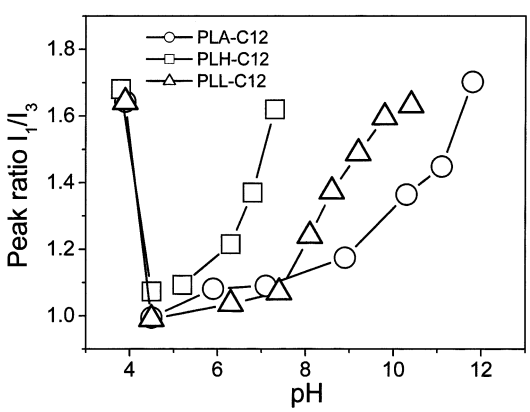

Fig. 6. Plot of the peak ratio I_I/I_{III} of the vibration fine structure for the emission of pyrene incorporated in PLA-C12 (circles), PLH-C12 (squares) and PLL-C12 nanoparticles (triangles) as a function of the pH value.

An increase of the I_I/I_{III} ratios was also found in the region of higher pH values. But it can be seen there that the pH dependent sensitivity of the I_I/I_{III} value in this region is the strongest for PLH-C12, medium for PLL-C12 and the lowest for PLA-C12. The increase is obviously in the same line as the pK_a values of the poly(amino acid). The microenvironment of pyrene becomes more and more polar with increased pH. It has about the same polarity of water when the pH is 7.3 (PLH-C12), 10.4 (PLL-C12) and 11.8 (PLA-C12). This is also consistent with the break-down of the complexes and the release of pyrene at higher pH values. The continuous increase of the I_I/I_{III} ratio at higher pH value can be ascribed to the water uptake of the nanoparticles. On the low and on the high side of the pH value, the I_I/I_{III} ratios increase drastically up to values of 1.65 to 1.70. At pH values below 4.3 the carboxylate becomes protonated to the acid, which then precipitates from the solution. The poly(amino acid)s remain uncomplexed in the solution. At pH values higher than the pK_a values of the poly(amino acid)s the ζ potentials of the particles decreases to 0 and the particles aggregate. At high pH values the poly(amino acid)s become deprotonated, the ionic bonding between the polymer and the fatty acid is destroyed and the pyrene is released into the aqueous surroundings when the particles expand and aggregate.

3.7. Secondary structures

The secondary structures of poly(amino acid)s are essentially a combination of α-helical, β-sheet and random coil segments. External parameters that affect them in connection with the present work are the pH value and the interaction with surfactants (Satake and Yang, 1973). It is well known that the amide groups of poly(amino acid)s show characteristic $\pi\pi^*$ and $n\pi^*$ transitions

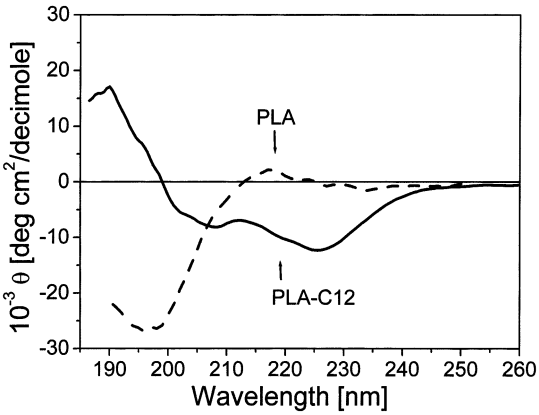

Fig. 7. Circular dichroism spectra of PLA (dashed line) and PLA-C12 (solid line) at pH 6.5. The curve of PLA with a characteristic minimum at 198 nm and a maximum at 218 nm results from a random coil conformation. By contrast, the curve of PLA-C12 with a maximum at 190 nm and the two minima at 208 and 224 nm results from a α-helical segments as predominant structure.

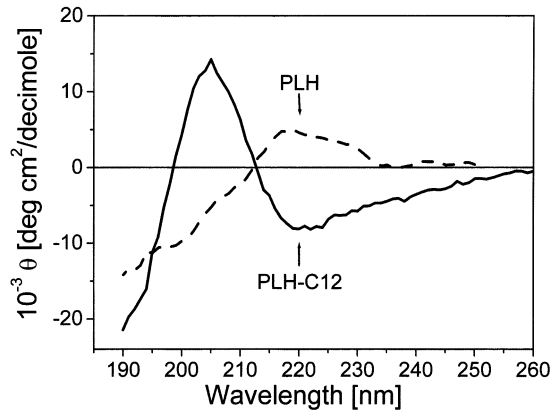

Fig. 8. Circular dichroism spectra of PLH (dashed line) and PLH-C12 (solid line) at pH 4.3. The curve of PLH with a minimum at 190 and a maximum at ~220 nm results from a random coil conformation while the two minima at 190 and 220 nm and the maximum at 205 nm in the curve of PLH-C12 result form β-sheet segments as the predominant secondary structure.

in their circular dichroism (CD) spectra that are sensitive to their secondary structures (Fasman, 1996). Circular dichroism measurements were carried out in order to determine whether the secondary structures of PLA, PLH and PLL differ from those of PLA-C12, PLH-C12 and PLL-C12, and further, whether the pH value influences complexed and uncomplexed poly(amino acid)s differently. Examples are shown in Fig. 7 (PLA, PLA-C12), Fig. 8 (PLH, PLH-C12) and Fig. 9 (PLL, PLL-C12). All spectra were measured at a temperature of 25 °C and in a pH regime in which the nanoparticles are stable. It can be seen that the CD spectra of PLA, PLH and PLL in their complexed states differ clearly from those in their uncomplexed states. The secondary structures of complexed and uncomplexed PLA, PLH and PLL are obviously different.

The CD curve of PLA at pH 6.5 (Fig. 7, dashed line) is characterized by a strong negative band at ~198 nm ($\pi\pi^*$ transition) and a small positive band at 218 nm ($n\pi^*$ transition). This spectrum is characteristic for a random coil structure, a finding which is consistent with the expectation that PLA has a random coil structure at pH 6.5, where it is positively charged. By contrast, it can be seen in Fig. 7 (solid line) that the PLA-C12 is characterized by a strong positive band at 190 nm ($\pi\pi^*_{\parallel}$ transition), and two weaker negative bands with maxima a about 208 nm ($\pi\pi^*_{\perp}$ transition) and 224 nm ($n\pi^*$ transition). This proves that the predominant structure of PLA-C12 is an α-helix at pH 6.5 and not a random coil as it is the case for

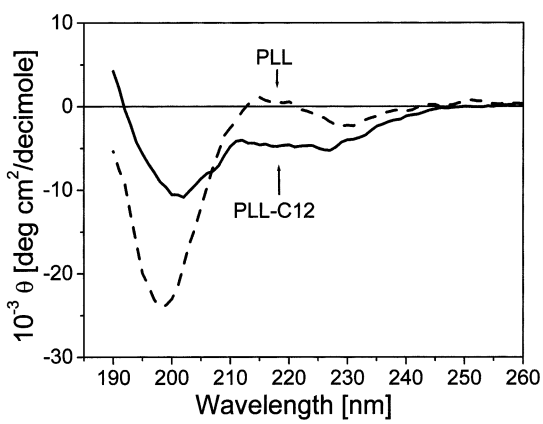

Fig. 9. Circular dichroism spectra of PLL (dashed line) and PLL-C12 (solid line) at pH 6.5. The characteristic minimum at 198 nm and the maximum at 218 nm in the curve of PLL results from a random coil conformation while the maximum at 190 nm and the two minima at ~208 and 224 nm in the curve of PLL-C12 result form a α-helical segments as the predominant secondary structure.

PLA. Tentatively, we interpret the presence of α-helices within the PLA-C12 complex as resulting from a stabilization of the α-helix due to the C12 moieties that are attached to the polymeric chains. Recently, we have made a similar observation for poly(ethylene oxide)-*block*-poly(L-lysine) complexes of retinoic acid (Thünemann et al., 2000), which show an enhanced stability of their α-helical PLL segments against lowering the pH of their surroundings.

Considering the corresponding pair PLH and PLH-C12 it can be seen in Fig. 8 that the CD curve of PLH (pH 4.3) is not as distinct as that of PLA. A clear maximum is, however, present at about 220 nm ($n\pi^*$ transition), the curve is negative below 210 nm and it has its lowest values around 190 nm ($\pi\pi^*$ transition). These characteristics are in agreement with the interpretation that the PLH chains are predominantly in a random coil conformation. By contrast, the CD spectrum of PLH-C12 (Fig. 8, solid curve) has a strong negative band at 190 nm, a positive band at 205 nm and a negative band at about 220 nm. This proves that significant amounts of β-sheets, which are characterized by a negative band near 215 nm ($n\pi^*$ transition) and positive band a 198 nm ($\pi\pi^*$ transition), are present in the PLH-C12 complex at a pH of 4.3. Random coil conformations dominate the PLH and β-sheets the PLH-C12. This is indicative for the preference of higher ordered secondary structures in the complex than in the pure polymer. It is probable that the higher ordered conformation allows for a better packing of the surfactants in the complexes. Finally, we considered the CD spectra of PLL and PLL-C12 at a pH 7.6 (Fig. 9, dashed and solid lines, respectively). It can be seen there that PLL, which shows a strong minimum at 198 nm ($\pi\pi^*$ transition) and a weak maximum in the range of 215–220 nm ($n\pi^*$ transition), is in a random coil stage. For the pure PLL the pH dependant conformational change from an α-helix (non-charged chains) to a random coil structure (positively charged chains) was determined to occur in range from pH 10.6 to 9.5 (not shown). Kataoka reported the same pH range for the conformational transition of PLL (Kataoka et al., 1996). In contrast to PLL the PLL-C12 show maximum values around 190 nm ($\pi\pi^*_{\parallel}$ transition), a pronounced minimum at 201 nm

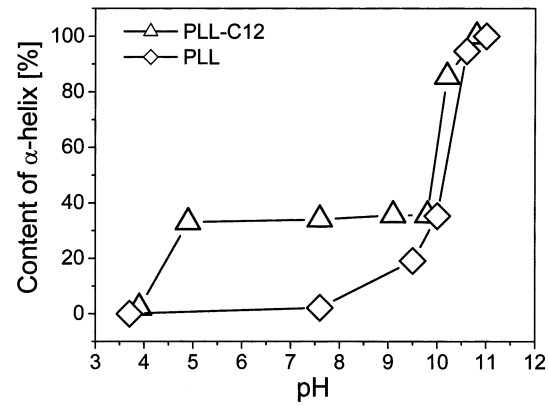

Fig. 10. Variation of the content of α-helices in the PLL-C12 nanoparticles (triangles) and the uncomplexed PLL (diamonds). PLL-C12 displays a high amount of α-helical segments at low pH values in contrast to pristine PLL.

($\pi\pi^*_{\perp}$ transition) and almost constant negative values in the range of 212 to 228 nm ($n\pi^*$ transition). For a first approximation we assume that the dominating structure elements of PLL-C12 are α-helical and random coil segments. The crossover wavelength, when varying the pH, remained at 204 nm. This agrees well with that of the pH-induced helix-coil transition of PLL and poly(ethylene oxide)-block-poly(L-lysine) reported in the literature (Greenfield and Fasman, 1969; Kataoka et al., 1996; Kataoka et al. 1998). A contribution of β-sheet structures to the spectra was not found. We concluded that the PLL conformation in the PLL-C12 adopts an α-helix for pH values higher than 10 and a random coil at a pH lower than 4.3, while between these limiting values a mixture of α-helical and random coil structures is present. According to Greenfield and Fasman (Greenfield and Fasman, 1969), the content of α-helices was estimated from the mean molar ellipticity at a wavelength of 222 nm. It can be seen in Fig. 10 that the α-helix content of PLL-C12 has nearly constant values of about 35% in the range of pH 4.8–9.8 whereas it is 0–20% for PLL. This finding is consistent with the interpretation that the chains are protected against conformational transitions as long as they are complexed. The chains that are located in the center of the cores of the nanoparticles are protected.

When the particles were dissolved, we were unable to determine significant differences between the conformations of PLL and PLL-C12. The stability of the α-helix within the complexes is remarkable when bearing in mind that the helix-coil transition of poly(L-lysine) homopolymers is found at pH 10.3 and 25 °C when the polymer is 35% charged (Chou and Scheraga, 1971) We assume that the α-helix of the complexes is stabilized by protecting dodecanoate molecules. This process ends when the dodecanoate moieties become protonated. This assumption is supported by the pK_a of dodecanoic acid that is ~ 4.9 (Small et al., 1986). It must be stated, though, that our simple evaluation of the content of the α-helix in PLL-C12 is not transferable to PLA-C12 and PLH-C12. This is probably due to the contributions of β-sheets and β-turns. The presence of more than two conformations can be verified by the fact that no isobestic point can be detected for PLA-C12 and PLH-C12 when the pH is varied. A summary of the predominantly secondary structures of the pure and complexed poly(amino acid)s as determined using the evaluation of the characteristic minima and maxima of their CD spectra while changing the pH value is given in Table 2.

Numerous attempts have been made in the literature to explain the contributions of the different structural elements. However a detailed interpretation of CD spectra, that would result in the quantitative assignment of the contributions of the different conformational segments is a difficult task. The results significantly depend, for example, on the evaluation method as has recently been discussed (Sreerama and Woody, 2000). The evaluation of the contributions of the different conformations to the CD spectra is a task that would need a comprehensive study of its own. At this point, we essentially restrict our interpretation to a qualitative discussion of the CD spectra.

4. Conclusions

We have presented the preparation of nanoparticles consisting of complexes of poly(L-arginine), poly(L-histidine) and poly(L-lysine) with dodecanoic acid. It was shown that the particles are of the core-shell type. The cores are formed by specific complexes and the shells are formed by uncomplexed polymeric chains. The structure of the core is relatively compact while that of the shell is diffuse and highly positively charged. It was also shown that the salt stability of the nanoparticles is high enough for drug delivery purposes and that their dissolution can be triggered by a change in the pH values. It was furthermore pointed out that the pH-sensitive ζ potentials and the dissolution properties of the particles correlate with the pK_a values of the poly(amino acid)s as well as with the pK_a value of dodecanoic acid. Using Q_{10} as a dopant for the nanoparticles it was also shown that up to 13% (w/w) Q_{10} could be incorporated into the particles without changing their properties. Information about the local surroundings of a hydrophobic dopant in the particles was

Table 2
pH-sensitivity of the predominant secondary structure of the poly(amino acid) chains in their complexed state as PLA-C12, PLH-C12 and PLL-C12 nanoparticles and those of the uncomplexed PLA, PLH, PLL

pH	PLA	PLA-C12	PLH	PLH-C12	PLL	PLL-C12
3.8	Random coil	Random coil	Random coil	Random coil	Random coil	Random coil
4.3	Random coil	α-helix + random coil	Random coil	β-sheet	Random coil	α-helix + random coil
5.4	Random coil	α-helix + random coil	β-sheet	β-sheet	Random coil	α-helix + random coil
6.8	Random coil	α-helix + random coil	–	–	Random coil	α-helix + random coil
10.2	Random coil	α-helix + random coil	–	–	α-helix	α-helix
11.2	Random coil	α-helix	–	–	–	–
12.4	β-sheet	–	–	–	–	–

–, cannot be assigned clearly.

obtained by using pyrene as a fluorescence probe. It was also suggested that the complexation of poly(amino acid)s by dodecanoic acids can result in a significant protection of the ordered chain conformations.

Acknowledgements

The authors would like to thank Marc Schneider for the AFM pictures, Ines Below and Dr Charl Faul for additional advice. We also gratefully acknowledge the financial support of the Deutsche Forschungsgemeinschaft (DFG-Schwerpunkt 'Polyelektrolyte mit definierter Molekülarchitektur', Grant Lo418/7-1), the Max Planck Society and the Fraunhofer Society.

References

Antonietti, M., Conrad, J., Thünemann, A.F., 1994. Polyelectrolyte-surfactant complexes—a new type of solid, mesomorphous material. Macromolecules 27, 6007–6011.

Bloomfield, V.A., 1991. Condensation of DNA by multivalent cations—considerations on mechanism. Biopolymers 31 (13), 1471–1481.

Boussif, O., Lezoualch, F., Zanta, M.A., et al., 1995. A versatile vector for gene and oligonucleotide transfer into cells in culture and in-vivo-polyethylenimine. Proc. Natl. Acad. Sci. USA 92, 7297–7301.

Buchhammer, H.-M., Petzold, G., Lunkwitz, K., 1999. Salt effect on formation and properties of interpolyelectrolyte complexes and their interactions with silica particles. Langmuir 15, 4306–4310.

Byk, G., Sherman, D., 2000. Genetic chemistry: Tools for gene therapy coming from unexpected directions. Drug Develop. Res. 50, 566–572.

Calvo, P., VilaJato, J.L., Alonso, M.J., 1997. Evaluation of cationic polymer-coated nanocapsules as ocular drug carriers. Int. J. Pharm. 153, 41–50.

Caruso, F., Donath, E., Möhwald, H., Georgieva, R., 1998. Fluorescence Studies on the binding of anionic derivatives of pyrene and fluorescein to cationic polyelectrolytes in aqueous solution. Macromolecules 31, 7365–7377.

Caruso, F., Möhwald, H., 1999. Protein multilayer formation on colloids through a stepwise self-assembly technique. J. Am. Chem. Soc. 121, 6039–6046.

Chou, P.Y., Scheraga, H.A., 1971. Calorimetric measurement of enthalpy change in isothermal helix-coil transition of poly-L-lysine in aqueous solution. Biopolymers 10, 657–680.

Dong, D.C., Winnik, M.A., 1982. The PY scale of solvent polarities—solvent effects on the vibronic fine-structure of pyrene. Fluorescence and empirical correlations with ET-value and Y-value. Photochem. Photobiol. 35 (1), 17–21.

Drummond, D.C., Zignani, M., Leroux, J.-C., 2000. Current status of pH-sensitive liposomes in drug delivery. Progr. Lipid Res. 39, 409–460.

Fasman, G.D., 1996. Circular Dichroism and the Conformational Analysis of Biomolecules, Plenum Press, New York.

Ferdous, A.J., Stembridge, N.Y., Singh, M., 1998. Role of monensin PLGA polymer nanoparticles and liposomes as potentiator of ricin A immunotoxins in vitro. J. Contr. Rel. 50, 71–78.

Gao, X., Huang, L., 1996. Potentiation of cationic liposome-mediated gene delivery by polycations. Biochem. USA 35, 1027–1036.

Goddard, E.D., 1986. Polymer surfactant interaction. 2. Polymer and surfactant of opposite charge. Colloids Surf. 19, 301–329.

Goddard, E.D., Ananthapadmanabhan, K.P., 1993. Interactions of surfactants with polymers and proteins. CRC Press, Boca Raton, FL, p. 22.

Greenfield, N., Fasman, G.D., 1969. Computed circular dichroism spectra for evaluation of protein conformation. Biochemistry 8, 4108–4115.

Hayagawa, K., Santerre, J.P., Kwak, J.C.T., 1983. Study of surfactant poly-electrolyte interactions—binding of dodecyltrimethylammonium and tetradecyltrimethylammonium bromide by some carboxilic poly-electrolytes. Macromolecules 16, 1642.

Hellweg, T., Henry-Toulme, N., Chambon, M., et al., 2000. Interaction of short DNA fragments with the cationic polyelectrolyte poly(ethylene imine): a dynamic light scattering study. Colloid Surfaces A 163, 71–80.

Hollas, M., Chung, M.-A., Adams, J., 1998. Complexation of pyrene by poly (allylamine) with pendant beta-cyclodextrin side groups. J. Phys. Chem. B 102 (16), 2947–2953.

Jada, A., Hurtrez, G., Siffert, B., Riess, G., 1996. Structure of polystyrene-block-poly(ethylene oxide) diblock copolymer micelles in water. Macromol. Chem. Phys. 197, 3697–3710.

Kalyanasundaram, K., Thomas, J.K., 1977. Environmental effects on vibronic band intensities in pyrene monomer fluorescence and their application in studies of micellar systems. J. Am. Chem. Soc. 99, 2039–2044.

Kataoka, K., Harada, A., Cammas, S., 1996. Stabilized alpha-helix structure of poly(L-Lysine)-block-poly(ethylene glycol) in aqueous medium through supramolecular assembly. Macromolecules 29, 6183–6188.

Kataoka, K., Ishihara, A., Harada, A., Miyazaki, H., 1998. Effect of the secondary structure of poly(L-lysine) segments on the micellization in aqueous milieu of poly(ethylene glycol)-poly(L-lysine) block copolymer partially substituted with a hydrocinnamoyl group at the *N*-position. Macromolecules 1998, 6071–6076.

Kawashima, Y., Yamamoto, H., Takeuchi, H., Hino, T., 2000. Mucoadhesive liposomes: physicochemical properties and release behavior of water-soluble drugs from chitosan-coated liposomes. STP Pharma. Sci. 10, 63–68.

Mast, R.C., Haynes, L.V., 1975. Use of fluorescent-probes perylene and magnesium 8-Anilinonaphthalene-1-sulfonate to determine critical micelle concentration of surfactants in aqueous-solution. J. Colloids Interface Sci. 53 (1), 35–41.

Muraoka, O., Ogiso, T., Koike, K., Iwaki, M., Tanino, T., Tanabe, G., 2000. Percutaneous penetration of ozagrel and the enhancement produced by saturated fatty acids. Biol. Pharm. Bull. 23, 844–849.

Nakamura, K., Osanai, S., 2000. Effects of complexation between liposome and poly(malic acid) on aggregation and leakage behaviour. Biomaterials 21, 867–876.

Philipp, B., Dawydoff, W., Linow, K.-J., 1982. Poly-electrolyte complexes. Z. Chem. 22, 1.

Ramsay, E., Birchall, J., Hadgraft, J., Gumbleton, M., 2000. Examination of the biophysical interaction between plasmid DNA and the polycations, polylysine and polyornithine, as a basis for their differential gene transfection in-vitro. Int. J. Pharm. 210, 97–107.

Remy, J.S., Pollard, H., Loussouarn, G., Demolombe, S., Behr, J.P., Escande, D., 1998. Polyethylenimine but not cationic lipids promotes transgene delivery to the nucleus in mammalian cells. J. Biol. Chem. 273, 7507–7511.

Satake, I., Yang, J.T., 1973. Effect of chain-length and concentration of anionic surfactants on conformational transitions of poly(L-ornithine) and poly(L-lysine) in aqueous-solution. Biochem. Bioph. Res. Co. 54, 930–936.

Schwarz, S., Buchhammer, H.M., Lunkwitz, K., Jacobasch, H.J., 1998. Polyelectrolyte adsorption on charged surfaces—study by electrokinetic measurements. Colloid. Surf. A 140, 377–384.

Seymour, L.W., Carlisle, R.C., Read, M.L., Wolfert, M.A., 1999. Self-assembling poly(L-lysine)/DNA complexes capable of integrin-mediated cellular uptake and gene expression. Colloid. Surface. B. 16, 261–272.

Small, Handbook of Lipid Research, Plenum Press, New York, 1986; vol. 4 (From Alkanes to Phospholipids), p. 602.

Sreerama, N., Woody, R.W., 2000. Estimation of protein secondary structure from circular dichroism spectra: comparison of CONTIN, SELCON, and CDSSTR methods with an expanded reference set. Anal. Biochem. 287, 252–260.

Tang, M.X., Szoka, F.C., 1997. The influence of polymer structure on the interactions of cationic polymers with DNA and morphology of the resulting complexes. Gene Ther. 4, 823–832.

Tedeschi, C., Möhwald, H., Kirstein, S., 2001. Polarity of layer-by-layer deposited polyelectrolyte films as determined by pyrene fluorescence. J. Am. Chem. Soc. 123, 954–960.

Thünemann, A.F., Beyermann, J., Kukula, H., 2000. Poly(ethylene oxide)-b-poly(L-lysine) complexes with retinoic acid. Macromolecules 33, 5906–5911.

Thünemann, A.F., General, S., 2001. Nanoparticles of a polyelectrolyte-fatty acid complex: carriers for Q_{10} and Triiodothyronine. J. Contr. Rel. 75, 237–247.

Thünemann, A.F., General, S., 2000. Poly(ethylene imine) *n*-alkyl carboxylate complexes. Langmuir 16, 9634–9638.

Tirrell, D.A., Linhardt, J.G., 2000. pH-induced fusion and lysis of phosphatidylcholine vesicles by the hydrophobic polyelectrolyte poly(2-ethylacrylic acid). Langmuir 16, 122–127.

Watanabe, K., Koyama, Y., Umehara, M., Mizuno, A., Itaba, M., Yasukouchi, T., Natsume, K., Suginaka, A., 1996. Synthesis of novel poly(ethylene glycol) derivatives having pendant amino groups and aggregating behavior of its mixture with fatty acid in water. Bioconjugate Chem. 7, 298–301.